

Short communication

Determination of strontium and lanthanum zirconates in YPSZ–LSM mixtures for SOFC

Claudia Alicia Cortés-Escobedo^{a,*}, Juan Muñoz-Saldaña^b,
Ana María Bolarín-Miró^c, Félix Sánchez-de Jesús^c

^a *Centro de Investigación e Innovación Tecnológica del IPN, Cda. Cecati s/n,
Col. Sta. Catarina, CP 02250, Azcapotzalco, D.F., Mexico*

^b *Centro de Investigación y Estudios Avanzados del IPN, Unidad Querétaro,
pdo. Postal 1-798, 76001 Querétaro, Qro., Mexico*

^c *Centro de Investigaciones en Materiales y Metalurgia, Universidad Autónoma del Estado de Hidalgo,
CU, Carr. Pachuca-Tulancingo Km. 4.5, Mineral de la Reforma, CP 42184, Hidalgo, Mexico*

Received 31 December 2007; received in revised form 30 January 2008; accepted 31 January 2008

Available online 8 February 2008

Abstract

Mixtures of 3% yttria- and partially-stabilized zirconia with LSM_x (strontium-doped lanthanum manganite, $x=0, 0.15$ and 0.2) were prepared and heat treated at temperatures between 1000 and 1300 °C to recreate the cathode–electrolyte interface interactions taking place during preparation and operation of solid oxide fuel cells (SOFC). Such interactions include the formation of La₂Zr₂O₇ and SrZrO₃, which are undesirable for SOFC. The effect of the manganese oxidation number on the mechanosynthesis of LSM during zirconate formation is also discussed. A quantitative analysis of zirconate formation by X-ray diffraction and Rietveld refinement was undertaken. Formation of lanthanum and strontium zirconates was completely avoided at temperatures as high as 1300 °C by synthesizing lanthanum manganites from MnO₂ doped with 15 at.% of Sr. Finally, in the presence of LSM, monoclinic phase content was diminished to less than 1.5 mol% after heat treatment at 1300 °C.

© 2008 Elsevier B.V. All rights reserved.

Keywords: Ceramics; Oxide materials; Fuel cells

1. Introduction

Lanthanum manganites (LaMnO₃), particularly those doped with strontium (La_(1-x)Sr_xMnO_{3±y} (LSM_x) with $x < 0.2$), are widely used as cathodes in solid oxide fuel cells (SOFCs). In these devices, yttria- and partially stabilized tetragonal zirconia (YPSZ) or fully-stabilized tetragonal zirconia (YSZ) is commonly used as the electrolyte due to its thermomechanical compatibility, adhesion and ionic conductivity [1–11]. A mixture of both materials in a 1:1 weight ratio increases adhesion and formation of O₂/LSM/zirconia triple phase boundaries (TPB), which is beneficial for molecular oxygen reduction [1,6,10]. An increase in the amount of TPBs increases cell efficiency. Several reports in the literature are devoted to increasing

the amount of TPBs, including an adaptation of a LSM cathode with a functional layer formed using the YSZ–LSM system and a YSZ layer as the electrolyte [1], or using a cathode formed only with a LSM–YSZ system [5,6,14]. The main problem of mixing lanthanum manganite with zirconia is the formation of La₂Zr₂O₇ (LZ) and SrZrO₃ (SZ) compounds, which have conductivities lower than those of LSM and YSZ [3,4,8,11–14]. These undesirable compounds are formed at temperatures as low as 800 °C due to lanthanum and strontium atomic diffusion in the structure of zirconia, thereby negatively affecting the cell efficiency. However, the mechanism governing formation of LZ and SZ is still under debate. Some authors found that strontium concentration in A-sites is a determining factor in LZ and SZ formation [2,14–17]. Chervin et al. [19] attribute LZ and SZ formation to Pt paste current collectors with bismuth flux in cells in operation. However, there are reports in which LZ and SZ compounds are not present after heat treatment at 1000 °C [10] or even 1400 °C [18] if monoclinic LSM is used. In other

* Corresponding author. Tel.: +52 55 57296000x64340; fax: +52 55 55617536.
E-mail address: ccortese@ipn.mx (C.A. Cortés-Escobedo).

reports, the presence of pyrochlores such as $(\text{La, Sr})_2(\text{Zr, Y})_2\text{O}_7$ has been found at 1400 °C, and has been accompanied by a cubic phase of zirconia [15].

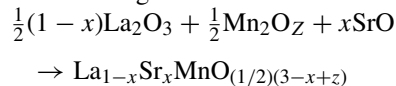
Different factors seem to affect the formation of LZ and SZ compounds, including the processing routes of the raw materials as well as the phase stability of zirconia. Mechanical alloying has been successfully used as a synthesis route for perovskite-like materials by processing them under non-equilibrium conditions. For instance, synthesis of lanthanum manganites by mechanical alloying with variations in oxidation state of the manganese ion was reported elsewhere [20,21]. These results can be compared with the change in the atom in A- or B- sites of the perovskite structure according to variation in oxidation state, as reported by Tsai et al. [6] and Ullman et al. [22].

The influence of the processing conditions during mechanosynthesis of LSM is still under investigation, as are the effects of the manganese oxidation number on formation of $\text{La}_2\text{Zr}_2\text{O}_7$ and SrZrO_3 and on the stability of LSM and ZrO_2 .

In order to evaluate the influence of the above parameters on the formation of zirconates in the TPBs, structural analysis by X-ray diffraction and the correspondent Rietveld pattern refinement were carried out in 1:1 mixtures of YSZ–LSM. LSM powders were synthesized from different oxidation states of manganese in LSM (MnO , Mn_2O_3 and MnO_2), with various concentrations of strontium in the A-sites of LSM (with $x=0$, 0.15 and 0.2).

2. Experimental

Lanthanum manganites were prepared by mechanosynthesis using precursor powders of La_2O_3 , Mn_2O_3 ($z=3$, Mn^{III}), MnO_2 ($z=4$, Mn^{IV}), SrO (Sigma–Aldrich) and MnO ($z=2$, Mn^{II} , Alfa Aesar) of 99.9 purity following the procedure reported elsewhere [20]. The reaction which represents the experimental results is the following:



Lanthanum manganite samples prepared by this method will be referred to hereafter as LSM_{xz} , where z is 2, 3 or 4 according to the oxidation number in the Mn-oxide precursor. The values of x are 0.15 or 0.20 for doping with 15% or 20% SrO, respectively. No value of x is given for undoped samples.

A SPEX 8000D mixer mill was used to mill the mixtures under atmospheric conditions with a 10:1 charge ratio, using steel as the milling medium.

Mixtures with $z=2$ were milled for 240 min and subsequently calcined at 1050 °C for 9 h in air. LM or LSM compounds with $z=3$ and 4 were obtained in a single step with 210 min and 270 min of milling, respectively. Manganites synthesized have a mixture of crystalline phases (cubic, orthorhombic and rhombohedral) even after calcining in air (1050 °C for 240 min), but rhombohedral structures predominate for $z=2$ and 3, and cubic structures dominate for $z=4$ [20]. This findings are in agreement with those results reported by Minh [23].

LM or LSM compounds were mixed with YPSZ (TZ3Y with 3 mol% of Y_2O_3 , TOSOH) with a tetragonal phase in a

1:1 (weight:weight) ratio. The powder mixtures thus obtained were uniaxially pressed at 700 MPa. The green samples were heat treated at 1000, 1100, 1200, and 1300 °C for 2 h in air at atmospheric pressure.

Structural analysis of sintered ceramics was carried out by X-ray diffraction (Rigaku D-MAX 2100 diffractometer) with $\text{Cu K}\alpha$ radiation ($\lambda = 1.5418 \text{ \AA}$) with 2θ ranging from 20° to 60° in increments of 0.02°. Rietveld refinement of the X-ray diffraction patterns was made by using MAUD 2.47 Software.

Finally, microstructural characterization of the heat-treated samples was carried out by scanning electron microscopy (Philips-XL30 ESEM) with backscattered electrons.

3. Results and discussion

Fig. 1 shows the X-ray diffraction patterns of mixtures of yttria- and partially-stabilized tetragonal zirconia (YPSZ) with lanthanum manganites synthesized from different Mn-oxide precursors (LM_z) without heat treatment (Fig. 1(a), (e) and (i)) and heat treated at 1300 °C (Fig. 1(b)–(d), (f)–(h) and (j)–(l)).

Fig. 1(a) and (b); (e) and (f); (i) and (j) corresponds to mixtures of YPSZ with undoped manganites prepared from Mn^{II} , Mn^{III} and Mn^{IV} , respectively. In these figures, increasing heat treatment temperature is shown to result in increased intensity and a widening of peaks. Further on, changes in the lanthanum manganite:tetragonal zirconia (LM:ZT) intensity ratio can be seen for samples obtained from Mn^{II} versus those obtained from Mn^{III} and Mn^{IV} in mixtures without heating. The main peak of LM from Mn^{II} is higher in intensity than the main peak of tetragonal zirconia; the LM in this particular case was obtained by calcination in air after ball milling, leading to larger grain size than was seen for the other manganites obtained by a single step of high-energy ball milling (see Fig. 1(a)) [20]. After heat treatment of this mixture, intensity of the main peak of LM from Mn^{II} becomes smaller than zirconia peak, indicating a transformation from the monoclinic phase to the tetragonal phase, as well as changes in grain sizes for both. More specifically, the lanthanum manganite grain size increases to a lesser extent than the zirconia grain size.

Fig. 1(c), (g) and (k) shows the X-ray diffraction patterns of lanthanum manganite with 15% strontium in lanthanum atomic sites synthesized from Mn^{II} , Mn^{III} and Mn^{IV} , respectively. All three samples were heat treated at 1300 °C. The X-ray diffraction patterns of lanthanum manganite with 20% strontium in lanthanum atomic sites (synthesized from Mn^{II} , Mn^{III} and Mn^{IV} heat treated at 1300 °C) are shown in Fig. 1(d), (h) and (l).

A comparison of the diffractograms in Fig. 1 allows a qualitative evaluation of the amount of lanthanum–strontium zirconates as a function of all the variables used, including the manganese oxidation number, the strontium doping concentration and the heat treatment temperature. Since the most critical aspect of these powders for SOFC applications is the avoidance of $\text{La}_2\text{Zr}_2\text{O}_7$ or SrZrO_3 compounds, one can easily observe that the tested powders present clear changes in the diffraction peaks associated with these phases. In order to quantify those changes, Rietveld refinement was performed in mixtures heat treated at temperatures between 1000 and 1300 °C. Results of

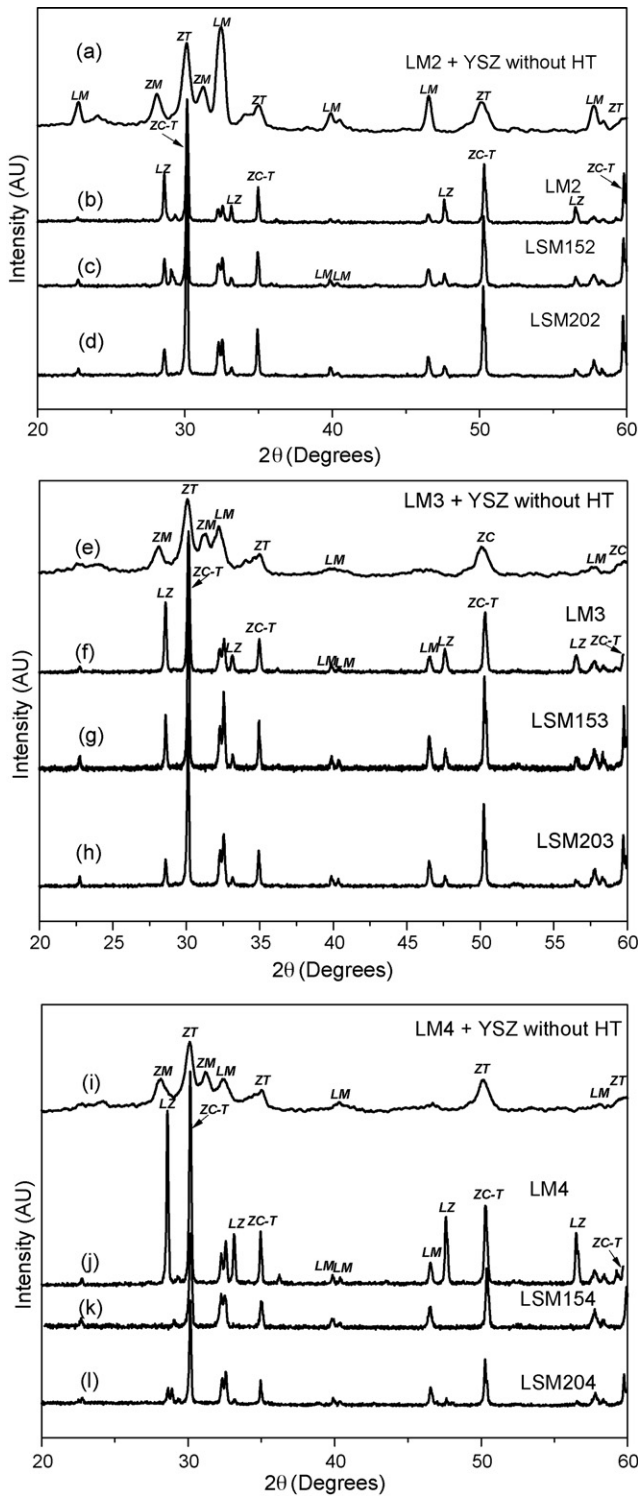


Fig. 1. X-ray diffraction patterns of mixtures of YPSZ with lanthanum manganites prepared from: (a)–(d) MnO, La₂O₃ and SrO by mechanosynthesis and calcinations in air; (e)–(h) Mn₂O₃, La₂O₃ and SrO by mechanosynthesis; (i)–(l) MnO₂, La₂O₃ and SrO by mechanosynthesis. Manganites in mixtures (a) and (b); (e) and (f); (i) and (j) are undoped. While manganites in mixtures (c), (g) and (k) are doped 15% of Sr in La sites and (d), (h) and (l) have 20% of Sr in La sites. All mixtures were heat treated at 1300 °C except (a), (e) and (i). These mixtures were not heat treated. ZM: monoclinic zirconia; ZC-T: cubic + tetragonal zirconia; ZT: tetragonal zirconia; LZ: lanthanum zirconate; LM: lanthanum manganite.

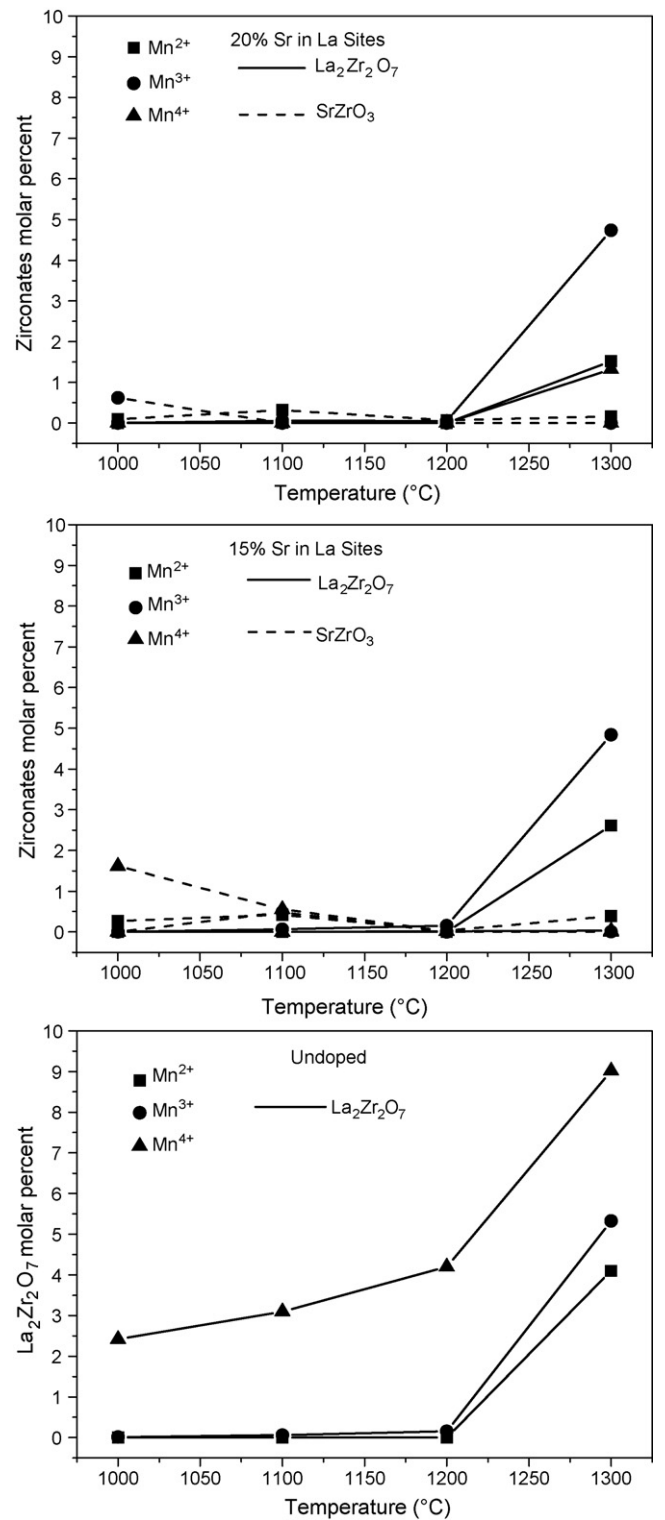


Fig. 2. Molar percent of monoclinic zirconia (*P21/c:1*) versus total zirconia in mixtures of YPSZ with lanthanum manganites (LSM) heat treated at temperatures from 1000 to 1300 °C (uncertainty: 0.71%).

refinements for $\text{La}_2\text{Zr}_2\text{O}_7$ pyrochlore and SrZrO_3 quantification are shown in Fig. 2. For the undoped manganites the highest content of lanthanum zirconate was observed for manganite obtained from Mn^{IV} precursor. This lanthanum zirconate content increases with the heat treatment temperature. Thus, undoped lanthanum manganites synthesized by high-energy ball milling are not suitable for SOFC applications. However, as mentioned before, avoiding formation of $\text{La}_2\text{Zr}_2\text{O}_7$ pyrochlore and SrZrO_3 in powders synthesized by this route is possible. For instance, doping the lanthanum manganites (prepared from Mn^{IV}) with 15% strontium in atomic lanthanum sites completely avoids the formation of lanthanum zirconate. However, the strontium zirconate content at 1000 and 1100 °C is highest for these mixtures. The best results are obtained from powders prepared with 20% atomic substitution of strontium in La sites. Only trace levels of strontium zirconate are present in these samples, and lanthanum zirconate appears only at 1300 °C. These results are important because it shows that doping of lanthanum manganites synthesized by high-energy ball milling is important for SOFC applications to avoid formation of lanthanum and strontium zirconates.

On the other hand, there are clear changes in the zirconia diffraction peaks due to the different conditions observed in Fig. 1. The most dramatic change is that the monoclinic phase present in YPSZ powders almost vanished completely after heat treatment for all the prepared mixtures at 1300 °C, irrespective of the oxidation number of the manganese ion. Results of the quantification by Rietveld refinement of the monoclinic phase versus the total zirconia molar content in each system are shown in Fig. 3. In all cases, there is a minimum zirconia monoclinic phase content at 1300 °C. Heat treatment of undoped manganites around 1100 °C leads to an increase in the monoclinic phase content versus the mixture heat treated at 1000 °C. This behavior may be related to the temperature of the monoclinic-to-tetragonal phase transformation reported by Scott [24]. A reduction in the monoclinic phase content leads to an increase in the cubic + tetragonal phase content.

This effect is different for manganites doped with strontium. Doping with 15% strontium in lanthanum atomic sites leads to a monotonic decrease in the monoclinic phase content as a function of temperature. Further, doping with 20% strontium in lanthanum sites shows an increase in the amount of monoclinic phase present at 1200 °C, then a decrease at 1300 °C. Further on, the oxidation number of manganese shifts the concentration of the monoclinic phase by forming lanthanum zirconate, contributing to the nonstoichiometry of lanthanum in manganites (A-site deficient). According to the results presented in this work, almost full stabilization of a high-temperature phase of zirconia (cubic $Fm\bar{3}m$, $a = 5.140078 \text{ \AA}$) plus tetragonal ($P42/nmc$, $a = 3.565 \text{ \AA}$, $c = 5.037 \text{ \AA}$) can be obtained using lanthanum manganite synthesized from Mn^{II} (mainly rhombohedral). For this system, the monoclinic phase is maintained below 10 mol%. Phase transformation from tetragonal to cubic phases is observed after heat treatment between 1100 and 1200 °C. For solid oxide fuel cell applications, the cubic phase of zirconia is more desirable, since there are no changes in structure or thermomechanical properties with variations in temperature.

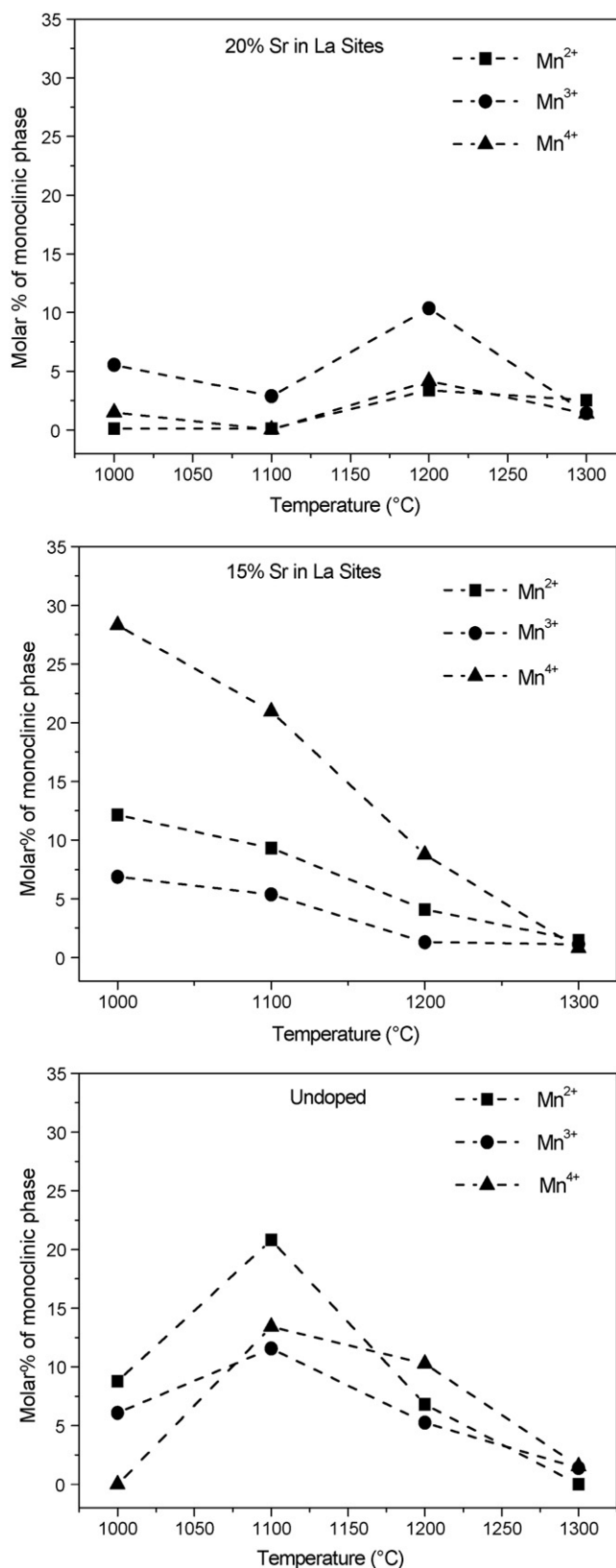


Fig. 3. Molar concentration of lanthanum ($Fd\bar{3}m:2$) and strontium ($I4mcm$) zirconates in mixtures of YPSZ with lanthanum manganites heat treated at temperatures from 1000 to 1300 °C (uncertainty: 0.71%). Straight and dashed lines represent lanthanum and strontium zirconate content, respectively.

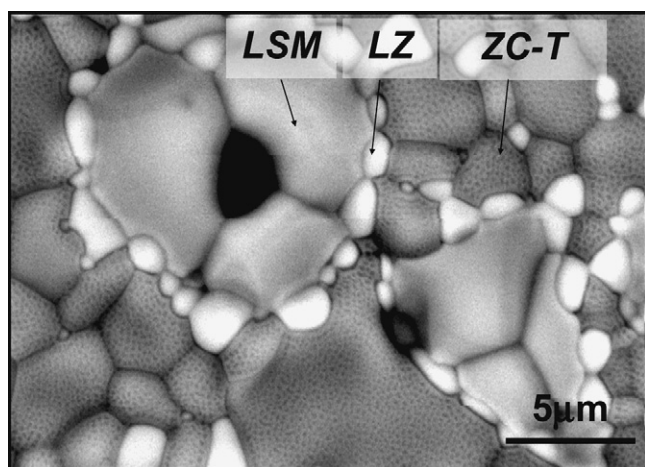


Fig. 4. SEM micrograph of the mixture of YPSZ with lanthanum manganite obtained from Mn^{II} undoped sintered at 1300°C .

A possible explanation for the difference in lanthanum zirconate content at 1300°C for the different samples is the charge balance—that is, the presence of Mn^{4+} promotes lanthanum diffusion into the zirconia structure, and the presence of Sr^{2+} stabilizes manganite structural charge if Mn^{4+} is predominant, but destabilizes structural charge if Mn^{3+} or Mn^{2+} is predominant. The nonstoichiometry in manganites is due to strontium content and oxidation number in manganese, and this nonstoichiometry generates mixtures of different lanthanum manganite phases (cubic, orthorhombic and rhombohedral) that simplify atomic diffusion and zirconate formation. A mixture of crystalline phases in manganites (cubic, orthorhombic and rhombohedral) still remains even after calcining in air without zirconia (1050°C for 240 min), but rhombohedral structures predominate for $z=2$ and 3, and cubic structures dominate for $z=4$. In all the X-ray patterns for LSM–YPSZ after heating, the presence of lanthanum manganite with mainly rhombohedral structure is observed. Singhal and Kendall [25] reported that transition metal oxides should form when lanthanum zirconate results from decomposition of lanthanum manganite in the presence of YSZ. This metallic oxide formation is substituted by a change in the oxidation number of manganese or in the lanthanum stoichiometry. Fig. 4 shows a representative micrograph of the mixture of YPSZ with undoped manganites after heat treatment at 1300°C . Phase transformation and grain growth is observed in the contrast given by the energy dispersion of the backscattered electrons from the different compounds—particles with bright, dark and intermediate contrasts correspond to $\text{La}_2\text{Zr}_2\text{O}_7$, ZrO_2 and lanthanum manganite, respectively. Moreover, the morphology of the cubic phase of zirconia, consisting of coarse grains with dots reported by Jiang et al. [15] related with manganese diffusion into cubic $(\text{Zr, Mn, Y})\text{O}_2$ alloy is observed. Based on the results of Jiang et al., who reported this morphology as a consequence of manganese oxide removal by acid washing from TZ3Y, and according to the Rietveld refinements results showed, grains with small dots were identified as cubic–tetragonal zirconia. Thus, grains which contrasted brightly and grains without dots were identified as lanthanum zirconate pyrochlore and lanthanum manganite, respectively. Based on these observations

and the grain morphologies, we can deduce the nature of the diffusion mechanisms. Grains of LZ present spherical convex edges from manganite to zirconia grains. Thus, diffusion of manganese ions occurs from LM to ZC-T in the liquid phase. On the other hand, changes in grain sizes are from about 0.5 to $5\ \mu\text{m}$ and from less than 1 to $4\ \mu\text{m}$ for lanthanum manganites and zirconia, respectively. The zirconate phase shows an average grain size of $1.2\ \mu\text{m}$.

In order to increase the cell efficiency in solid oxide fuel cells, it is convenient to maximize the ionic conductivity, especially at the cathode–electrolyte interface. To do this, an increase in triple phase boundaries is required. Since the size of the powders processed by mechanosynthesis of lanthanum manganites is of the order of a few hundreds of nanometers, the obtained LM powders should present high surface area and kinetic activity. In the same way, for those mixtures, where the formation of La and Sr zirconates was avoided, an increase of the TPBs amount at the interface with zirconia is also expected. Based on this, we would expect that for cathodes in fuel cell applications, the best option is the use of LSM obtained from Mn^{IV} and with 15 at.% of strontium in lanthanum sites. Our experimental results support this hypothesis, since the smallest quantity of lanthanum zirconate was found for these mixtures at all temperatures.

4. Conclusions

Formation of lanthanum and strontium zirconates at temperatures as high as 1300°C was diminished in lanthanum manganites synthesized by mechanosynthesis from mixtures with Mn^{IV} and doped with 15 at.% of strontium. Moreover, the highest content of lanthanum zirconate was found in undoped manganites. The amount of Sr as a dopant and the oxidation number of Mn for the preparation of lanthanum manganites by mechanosynthesis are important factors to prevent formation of zirconates. In fact, the last is the most important factor to avoid LZ formation at high temperature for LM–YSZ mixtures. The smallest quantity of monoclinic zirconia in the whole range of temperatures studied was for lanthanum manganite prepared from Mn^{IV} . The morphology of sintered mixtures indicates that zirconia is in the cubic phase, but deconvolution indicates a mixture of tetragonal + cubic phases. This also favors its use in SOFCs, since cubic zirconia does not suffer any changes over a wide range of temperatures.

Acknowledgment

Support of this work by the CONACyT-Mexico is gratefully acknowledged.

References

- [1] V.A. Haanappel, C.J. Mertens, D. Rutenbeck, C. Tropicz, W. Herzhof, D. Sebold, F. Tietz, J. Power Sources 14 (2005) 216.
- [2] C.-C.T. Yang, W.-C.J. Wei, J. Am. Ceram. Soc. 87 (2004) 1110.
- [3] J. Mc Evoy, Solid State Ionics 132 (2000) 159.
- [4] J. Mc Evoy, Solid State Ionics 135 (2000) 331.
- [5] E.P. Murray, T. Tsai, S.A. Barnett, Solid State Ionics 110 (1998) 235.
- [6] T. Tstai, S.A. Barnett, Solid State Ionics 93 (1997) 207.

- [7] H. Taimatsu, K. Wada, H. Kaneko, H. Yamamura, J. Am. Ceram. Soc. 75 (1992) 401.
- [8] H. He, Y. Huang, J. Regal, M. Boaro, J.M. Vohs, R.J. Gorte, J. Am. Ceram. Soc. 87 (2004) 331.
- [9] A. Labrincha, L.J. Meng, M.P. dos Santos, F.M.B. Marques, J.R. Frade, Mater. Res. Bull. 28 (1993) 101.
- [10] Z.V. Marinković, L. Mančić, J.-F. Cribier, S. Ohara, T. Fukui, O. Milošević, Mater. Sci. Eng. A 375 (2004) 615.
- [11] K.C. Wincewicz, J.S. Cooper, J. Power Sources 140 (2005) 280.
- [12] O.A. Shlyakhtin, Y.J. Oh, J. Mater. Chem. 12 (2002) 2486.
- [13] M.C. Brant, L. Dessemond, Solid State Ionics 138 (2000) 1.
- [14] M. Juhl, S. Primdahl, C. Manon, M. Mogense, J. Power Sources 61 (1996) 173.
- [15] S.P. Jiang, J.P. Zhang, K. Föger, J. Eur. Ceram. Soc. 23 (2003) (1865).
- [16] K. Wiik, C.R. Schmidt, S. Faaland, S. Shamsili, M.A. Einarsrud, T. Grande, J. Am. Ceram. Soc. 82 (1999) 721.
- [17] K. Kleveland, M.A. Einarsrud, C.R. Schmidt, S. Shamsili, S. Faaland, K. Wiik, T. Grande, J. Am. Ceram. Soc. 82 (1999) 729.
- [18] A.K. Sahu, A. Ghosh, A.K. Suri, P. Sengupta, K. Bhanumurthy, Mater. Lett. 58 (2004) 3332.
- [19] C. Chervin, R.S. Glass, S.M. Kauzlarich, Solid State Ionics 176 (2005) 17.
- [20] C.A. Cortés Escobedo, F. Sánchez de Jesús, A.M. Bolarín Miró, J. Muñoz-Saldaña, J. Phys. Status Solidi C 4 (2007) 4254.
- [21] M. Muroi, R. Street, P.G. Mc Cormick, J. Solid State Chem. 152 (2000) 503.
- [22] H. Ullmann, N. Trofimenko, F. Tietz, D. Stöver, A. Ahmad-Khanlou, Solid State Ionics 138 (2000) 79.
- [23] N.Q. Minh, J. Am. Ceram. Soc. 76 (1993) 563.
- [24] H.G. Scott, J. Mater. Sci. 10 (1975) 1527.
- [25] S.C. Singhal, K. Kendall, High Temperature Solid Oxide Fuel Cells—Fundamental Designs and Applications, Elsevier, Amsterdam, 2003.